The pinch-off process in a starting buoyant plume

T. S. Pottebaum, M. Gharib

Abstract The vortex ring formation process of a starting buoyant plume was studied experimentally using digital particle image thermometry and velocimetry (DPITV). The vortex ring was observed to pinch-off, or become disconnected, from the trailing plume. Pinch-off occurred at non-dimensional times, or formation numbers, between 4.4 and 4.9. The observed pinch-off process is consistent with an explanation based upon the Kelvin–Benjamin variational principle. This is analogous to the pinch-off of a vortex ring generated using a piston–cylinder apparatus, suggesting that pinch-off is a general component of the vortex ring formation process for various generation mechanisms.

1
Introduction

1.1
Starting buoyant plume

The starting buoyant plume is a basic convection phenomenon that occurs in a wide variety of circumstances. The source of energy for a starting plume is the distribution of mass in a gravity field—available gravitational potential energy is converted into kinetic energy as mass is redistributed to minimize the total potential energy of the system. Starting buoyant plumes are central to many environmental flows, such as cloud formation, discharge of volcanic gases and the release of pollutants from industrial and military sites. They are also the building blocks of more complicated processes, like heat transfer from horizontal boundaries and the Rayleigh–Taylor instability.

Turner (1962) introduced the term "starting plume" to distinguish this type of flow from both steady plumes and buoyant vortex rings (thermals). Steady plumes are the convection driven by a continuous source of buoyancy. Thermals, in contrast, are the result of the sudden release or production of a finite amount of buoyant fluid. As a starting plume develops, a cap forms that contains a vortex

ring similar to a thermal. Behind the cap, there is a stem or trailing plume that resembles a steady plume. Turner (1962) modeled the starting buoyant plume by assuming that the cap moves with some fixed fraction of the steady plume velocity at the same height, and then calculated the flux of buoyancy and momentum from the stem to the cap using the solution for a steady plume. The specific models of a steady plume and of a buoyant vortex ring were taken from Morton et al. (1956) and Turner (1957). This starting plume model captures the essential difference between a thermal and the vortex ring that forms as the cap of a starting plume—the fluid entrained by the cap from the rear is fluid from the stem, while a thermal entrains ambient fluid. Additional works on starting buoyant plumes are reviewed by Fay (1973) and List (1982).

More recently, detailed experiments have been conducted to measure the properties of the starting plume directly. Tanny and Shlien (1986) measured the velocity field in a starting plume by tracing particle paths in long exposure photographs. They found that vorticity in the cap was diffused, with no distinct core. Chay and Shlien (1986) measured the scalar field (temperature or concentration) in starting buoyant plumes using interferograms, and they found that the scalar distribution depends on the Prandtl number. Lundgren et al. (1992) conducted experiments and computations of a downburst, and presented scaling arguments to extend their results to atmospheric flows. Their experiments indicate that the cap velocity is constant over a large period of time. From their computations, the authors were able to present time resolved position and circulation data for the cap of the downburst. Moses et al. (1993) studied the scaling laws applicable to the cap. Though they used encapsulated thermochromic liquid crystal particles to visualize the starting plume, they did not extract quantitative temperature or velocity data.

1.2
Vortex ring pinch-off

Gharib et al. (1998) performed a series of experiments with vortex rings produced using a piston–cylinder apparatus. They found that there exists a maximum circulation that the vortex ring can attain, and any additional circulation produced by the apparatus ends up in a trailing jet. The critical parameter for this pinch-off process was identified as the "formation number," a non-dimensional time that is equivalent to the stroke ratio, L/D, where L is the distance traveled by the piston and D is the cylinder diameter. Gharib et al. (1998) showed that for formation numbers less than about 4, all of the circulation produced by the

T. S. Pottebaum (✉), M. Gharib
Graduate Aeronautical Laboratories,
California Institute of Technology,
M/C 205–45, Pasadena, CA 91125, USA
E-mail: tpotteba@caltech.edu
Tel.: +1-626-3954462
Fax: +1-626-5775258

piston motion became part of the vortex ring, while for larger formation numbers a trailing jet existed.

The authors also showed that this pinch-off process is consistent with the Kelvin–Benjamin variational principle (Kelvin 1880, Sects. 4 and 18; Benjamin 1976), which states that a steady, translating vortex ring has maximum energy with respect to impulse-preserving, iso-vortical (i.e., the circulation of each fluid element is preserved) perturbations. When a vortex ring is perturbed by the entrainment of additional vorticity, the vorticity must be redistributed to form a new vortex ring. In this redistribution process, the added vorticity can either be incorporated into the new vortex ring or expelled from the vortex ring in order to maximize the energy. Detailed models of this pinch-off process were later developed (Mohseni and Gharib 1998; Shusser and Gharib 2000a) based upon the Kelvin–Benjamin variational principle. In these models, pinch-off is taken to occur when the fluid delivered by the trailing jet, though it carries additional circulation, has insufficient energy to sustain a steady vortex ring.

While indirect evidence for vortex ring pinch-off in starting buoyant plumes exists in earlier studies (Fernando et al. 1998; Rast 1998), this process was first explicitly addressed by Johari and Gharib (1998). They performed experiments with buoyant fluid released from a cylindrical tube. A starting vortex ring was initially formed, but the pinch-off process could not be observed because the apparatus resulted in a thermal, not a starting plume.

Shusser and Gharib (2000b) continued the study of pinch-off in starting buoyant plumes. They demonstrated that the characteristic time used by Gharib et al. (1998) is equivalent to the time scale for a downburst used by Lundgren et al. (1992). The authors then presented a model that predicts vortex ring pinch-off in a starting buoyant plume.

Lundgren et al. (1992) defined the characteristic time scale for vortex ring formation in downbursts (cold thermals) as

$$T_0 = \left(\frac{R_0\rho}{g\Delta\rho}\right)^{\frac{1}{2}} \tag{1}$$

where R_0 is the equivalent spherical radius of the parcel of fluid, ρ is the density of the downburst parcel, $\Delta\rho$ is the difference between the downburst parcel density and the ambient density, and g is acceleration due to gravity. The characteristic time for vortex ring formation by a piston–cylinder apparatus was defined by Gharib et al. (1998) as

$$T_1 = D/U_{\mathrm{p}}, \tag{2}$$

where D is the cylinder diameter and U_{p} is the average piston velocity. Stated more generally, this definition takes the characteristic time, T_1, to be the ratio of the characteristic length to the characteristic velocity. Assuming that the plume width is approximately the diameter of the initial parcel of buoyant fluid, the characteristic length for the starting plume is $2R_0$. The characteristic velocity is not as simple to define because the starting plume has a buoyancy source, not a momentum source like the starting jet. Therefore, Shusser and Gharib (2000b) take the characteristic velocity to be the velocity acquired by a parcel of buoyant fluid initially at rest after traveling one characteristic length subject only to the buoyancy force. The buoyancy force produces a constant acceleration, $g\Delta\rho/\rho$, which can be integrated in time to yield

$$v = (g\Delta\rho/\rho)t$$

and

$$\Delta z = \frac{1}{2}(g\Delta\rho/\rho)t^2$$

where v is the velocity acquired, Δz is the vertical distance traveled and t is time. Taking $\Delta z = 2R_0$ and eliminating the time results in a characteristic velocity

$$V = \sqrt{4R_0 g\Delta\rho/\rho}. \tag{3}$$

The ratio of characteristic length to characteristic velocity then becomes

$$\frac{2R_0}{V} = \sqrt{\frac{R_0\rho}{g\Delta\rho}}, \tag{4}$$

which is equal to Lundgren et al.'s (1992) time scale in Eq. 1. Because the pinch-off time for piston–cylinder generated vortex rings collapsed well using the definition in Eq.2 for the characteristic time, it is expected that Lundgren et al.'s (1992) time scale is the proper scaling to use in studying the pinch-off process in a starting plume.

Shusser and Gharib (2000b) also developed a model for the pinch-off process in a starting plume by applying the Kelvin–Benjamin variational principle. The authors modeled the growth of both the stem and the cap of the starting plume, accounting for the fluxes between the two. The properties of the vortex ring after pinch-off were inferred from the data of Lundgren et al. (1992) rather than being calculated directly in the model. The various non-dimensional quantities used in the current study are those defined by Shusser and Gharib (2000b) as

$$\tau = \frac{t}{T_0}, \quad \zeta = \frac{z}{R_0}, \quad m = \frac{M}{M_0}, \quad i = \frac{IT_0}{M_0 R_0}, \quad e = \frac{ET_0^2}{M_0 R_0^2},$$

$$\gamma = \frac{\Gamma T_0}{R_0^2}, \quad \text{and } u = \frac{UT_0}{R_0} \tag{5}$$

where t is the time, z is the vertical coordinate, M is the mass of the cap, I is the impulse, E is the kinetic energy, Γ is the circulation, and U is the velocity in the z direction. The characteristic mass, M_0, is related to the mass of buoyant fluid in a hemisphere with radius R_0, such that $M_0 = \pi\rho R_0^3$, where ρ is now the density of the initial parcel of buoyant fluid.

Because the Kelvin–Benjamin variational principle is applicable to impulse-preserving iso-vortical perturbations, Shusser and Gharib (2000b) also defined a non-dimensional energy

$$\alpha = \frac{E}{\sqrt{\rho\Gamma^3}} = e\sqrt{\frac{\pi}{i\gamma^3}}, \tag{6}$$

as was done by Shusser and Gharib (2000a) and similar to what was done by Gharib et al. (1998). Pinch-off is predicted to occur at the time when α for the stem becomes less than α for the cap of the starting plume. The authors calculate that pinch-off occurs at a non-dimensional time, or formation number, $\tau \approx 4.73$. They also note that the cap velocity exceeds the stem velocity at $\tau \approx 4.46$ and this can be taken as an approximation of the pinch-off time.

1.3
Digital particle image thermometry and velocimetry
Digital particle image thermometry and velocimetry (DPITV) is a combination of two techniques that allows the temperature field and the velocity field to be measured simultaneously in a thin cross-section of a flow. Digital particle image velocimetry (DPIV) is a technique for determining the velocity field from consecutive images of particles suspended in a flow. Digital particle image thermometry (DPIT) refers to the extraction of temperature field information from the color of thermochromic liquid crystal (TLC) particles, which change their reflected wavelength with temperature. DPITV combines these two techniques by using the TLC particles as both temperature indicators and flow tracers.

DPITV is accomplished by seeding a flow with TLC particles, illuminating a cross-section with a pulsed sheet of white light, and digitally recording color images of the illuminated particles. The intensity field of the images, i.e., the black and white image left when color information is removed, is used to determine the velocity field through standard DPIV algorithms. The color information in the images is used to determine the temperature field.

DPIV is the digital version of the particle image velocimetry technique and was first used by Willert and Gharib (1991). DPIV processing techniques have progressed since this initial implementation, but the central idea remains unchanged. Cross-correlations of small windows in consecutive images produce displacement estimates, which are converted to velocities using the known time separation between images. A comparison of widely used DPIV processing techniques can be found in McKenna and McGillis (2002).

DPIT depends upon the property of TLC that they selectively reflect light of a particular wavelength. The TLC acts as a Bragg scattering volume grating with a temperature dependant pitch. The apparent color of the TLC therefore depends on the temperature and on the angle between the incident light and the observer. Because the relationship between color and temperature is sensitive to chemical composition and to the optical arrangement, it is necessary to calibrate TLC for use in experiments. A complete discussion of the optical and chemical properties of TLC can be found in Parsley (1991).

TLC has been used extensively for measuring temperature on surfaces. The first reported use of TLC applied to a surface for fluid mechanics research was in a qualitative study by Klein (1968). More recently, TLC has been used to seed fluid flows in order the measure the temperature field within the flow. Rhee et al. (1984) pioneered this use, though their results were only qualitative. The DPIT technique in its present form was introduced by Dabiri

and Gharib (1991) and was used to investigate the wakes of heated cylinders by Park et al. (2001).

The quantitative measurement of temperature fields using TLC has advanced considerably in recent years. Park (1998, Sect. 2.3) presents a review of various color decomposition schemes used for TLC calibration. According to Park et al. (2001), the uncertainty in temperature for individual TLC particles is 5–20% of the useful temperature range. A range of uncertainties is used because the calibration curve is non-linear, so the uncertainty varies over the useful temperature range. For 32×32 pixel averaging windows, this uncertainty is reduced to 2–10%.

2
Experimental details

2.1
Setup
In this experiment, an electrical heater located at the bottom of a temperature-controlled tank produced a starting buoyant plume. The velocity and temperature fields were measured using DPITV. Figure. 1 shows a sketch of the overall setup.

The tank consisted of two separate regions. The starting plume was produced in the inner region, which had a square cross-section measuring 133 mm on each side. It was filled to a depth of 216 mm with a 15% (by volume) glycerol solution. The fluid was seeded with 100-μm dia. encapsulated TLC particles (BM100R26C20 W, Hallcrest Inc., Glenview, IL, USA) with the same density as the glycerol solution. The thermal response time of the TLC particles was approximately 4 ms (Dabiri and Gharib 1991). The useful temperature range for these TLC particles in right-angle viewing was 25.8–28.0°C.

At the base of the tank's inner region, a 12.7 mm dia. disk of 0.127-mm thick copper sheet was set flush with the tank bottom. A round thermofoil heater (HK5537R3.8L12E, Minco Products Inc., Minneapolis, MN, USA) was bonded to the external side of the copper disk and was powered using a variable DC power supply (BOP 50–4M, Kepco Inc., Flushing, NY, USA). The diameter of the heated disk was used as the characteristic length scale for the starting plume, $2R_0$. The measured width of the starting plume agreed well with this dimension.

The outer region of the tank, with sides measuring 292 mm, was used to control the temperature. Tap water was continuously cycled between the outer region and a recirculating temperature controller (Neslab RTE-110, Thermo Electron Corp., Waltham, MA, USA). All of the tank walls were 3.18 mm thick acrylic plastic, and a 6.35 mm thick acrylic plastic lid was placed over both regions. Additionally, a section of 6.35 mm thick acrylic plastic was suspended at the surface of the inner tank.

The starting plume was illuminated with a vertical sheet of pulsed white light passing over the center of the heating disk. In the region containing the plume, the sheet thickness varied between 1 and 3 mm. The white light sheet was produced using a pair of xenon flash tubes. The flash tubes were arranged with a reflector so that the sheet produced by either tube appeared to originate from the same location. The flash tubes were fired alternately to achieve the
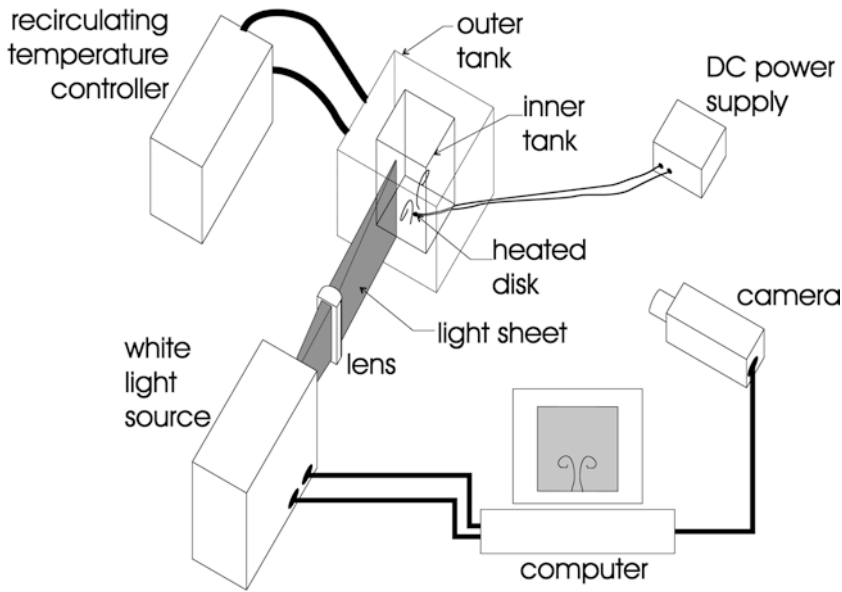
Fig. 1. Sketch of the experimental setup

desired mean pulse separation. Variation in the pulse separation, owing to the triggering mechanism's sensitivity to the temperature and ionization state of the xenon gas, is a significant source of scatter in the velocity measurements. Images for DPITV were captured using a 3CCD color video camera (DXC-9000, Sony Business Solutions & Systems Co., Park Ridge, NJ, USA) and recorded directly to computer hard disk. Images were recorded in pairs 45 ms apart at a rate of 15 pairs/s. The camera was located approximately 2 m from the illuminated plane and imaged an area 97.6 mm high by 73.6 mm wide.

2.2
Procedures
Experiments were conducted with a background temperature of 25.8°C. One experimental run consisted of starting to record images, then applying a constant voltage to the heating element for a fixed time interval. When the resulting vortex ring left the camera's field of view, the recording was stopped. Following each run, the fluid was stirred and allowed to settle for at least 15 min before the next run.

The applied voltage and time interval were adjusted by trial and error to obtain useful data. In order to allow quantitative temperature information to be extracted from the DPITV data sets, the maximum temperature in the flow was kept within the useful range of the TLC's, and care was taken to insure that the temperature differences did not cause large index of refraction changes. Based on these temperature criteria and on the need to observe the plume with sufficient spatial and temporal resolution, a temperature difference of 0.9±0.05°C, corresponding to a density ratio $\Delta\rho/\rho$=0.00026±0.00001, was used. This yielded a characteristic time, T_0, of 1.59±0.04 s. Three separate runs were conducted at these conditions.

2.3
TLC calibration
Calibration of the TLC particles was performed directly in the water tank under the same lighting and viewing conditions as the experiment. A new calibration was

performed each day that data was collected. For calibration, the water in the outer tank was chilled to 18°C while the inner tank temperature was actively controlled. A propeller, a reference thermometer (2180A, Fluke Corp., Everett, WA, USA), the temperature controller probe (PTC-41, Tronac Inc., Oram, UT, USA), and a cylindrical heating rod were suspended in the inner tank for calibration, but removed when running the experiment. Starting at 25.3°C, the temperature was set to increasing temperatures in approximately 0.1°C increments up to 28.0°C. About 1 min was required for the tank to reach a uniform, steady temperature at each calibration point. At each temperature, 10 images were recorded.

Color was determined in the hue-saturation-intensity color space. The hue of each particle was determined, and then the hues of all particles at a particular temperature were averaged. A sixth order polynomial least-squares curve fit relating hue to temperature was constructed, which was later used to determine temperature from the DPITV data sets.

2.4
Processing
The velocity field was determined by applying standard DPIV algorithms to black and white intensity images extracted from the DPITV data. The data was processed using 32×32 pixel interrogation windows with 50% overlap. The resulting velocity vectors are $0.39R_0$ apart. Window shifting was used to reduce errors associated with in-plane particle loss. The stream function (ψ) and the vorticity (ω) field were then calculated from the velocity field.

The intensity images were also used to locate individual particles as the first step in determining the temperature field. Each particle was assigned a hue based upon the average hue of the brightest pixel and its eight closest neighbors, excluding those pixels with saturation below a fixed threshold. To produce a temperature field on a structured grid, particle hues were averaged in 32×32 pixel windows corresponding to the DPIV interrogation windows. The density (ρ) field was then determined using the

temperature field and the known equation of state for the mixture. The density at the center of the initial region of buoyant fluid was used to calculate the density ratio for the experiment.

The kinetic energy E, impulse I and circulation Γ of the starting plume and vortex ring were computed using summations to approximate the integrals

$$E = \pi \iint \rho \omega \psi \, \mathrm{d}z \mathrm{d}r, \quad I = \pi \iint \rho \omega r^2 \mathrm{d}z \mathrm{d}r, \quad \Gamma = \iint \omega \mathrm{d}z \mathrm{d}r.$$
(7)

A contour of absolute value of vorticity of 0.45 s^{-1} was used as the boundary of the integrals. This vorticity contour was selected because it enclosed the majority of the vorticity in the flow while allowing the vortex ring to be clearly distinguished from the trailing plume. Over a range of reasonable values for the bounding vorticity contour, the results of the measurements do not vary significantly. After locating the bounding vorticity contour, the integrand was summed for all points lying inside the contour. Points lying exactly on the contour were also included, but with a weight factor of 0.5. Except at late times, it is not possible to separate the vortex ring from the trailing plume using a reasonable vorticity contour. Therefore, the circulation, impulse and energy of the vortex ring and of the trailing plume cannot be measured independently near the pinch-off time.

Care was taken in determining the start time of each buoyant plume. There is no external trigger that indicates when the experiment begins—the time at which power is applied to the heating element is not the start time because motion of the buoyant fluid does not immediately begin. This is in contrast to experiments in which fluid of a different density is released at a known time (Lundgren et al. 1992; Johari and Gharib 1998). Shusser and Gharib (2000b) assume that the buoyant fluid is created instantaneously at $t=0$ and motion of the fluid then immediately commences. To be consistent with this definition of the start time, in this study $t=0$ is taken to be one video frame prior to the first observable velocity above the noise level at the heating disk. Even though heated fluid exists prior to this time, it is assumed that motion of the fluid is negligible because of the relatively large viscosity. This method may cause a systematic offset of τ by ±0.02.

3
Results
Figure 2 shows snapshots of the starting plume at four equally spaced times from a single run. The images (contrast and intensity enhanced) are shown along with the corresponding instantaneous vorticity and temperature fields. At early times, the cap and stem are intimately connected, and it is not possible to distinguish where one ends and the other begins. At late times, the vortex ring and trailing plume are clearly separated, with a region of fluid at ambient temperature and low vorticity existing between them.

Figure 3 shows the non-dimensional circulation of the total starting plume and of the pinched-off vortex ring as functions of time for the same run as the snapshots in

Fig. 2. The vortex ring data includes only those points taken at late times. This is because, as mentioned previously, it is difficult to distinguish the vortex ring from the plume at earlier times. The total circulation in the stem plus the cap increases with time throughout the experiment. For the vortex ring alone, at late times the circulation maintains an approximately constant value, with $\gamma=5.3\pm0.5$ for this run. For this run, the total circulation in the starting plume is equal to the vortex ring circulation at a time of $(4.8\pm0.7)T_0$. Following Gharib et al. (1998), this is taken to be the pinch-off time or formation number, $\tau_{\mathrm{pinch\text{-}off}}$. The impulse i, and kinetic energy e, of the total plume also increased with time.

In contrast, the non-dimensional energy α for the total plume decreased with time. Figure 4 shows α as a function of time for the total plume and for the vortex ring alone in the same run as in the previous figures. At late times, the vortex ring maintained a constant value of α. The total plume non-dimensional energy, α_{tot}, drops below the late time vortex ring value, α_{vr}, at a non-dimensional time of around 3.5, which is well before the pinch-off time. For the three runs, α_{tot} fell below α_{vr} between $1.2T_0$ and $1.4T_0$ prior to $\tau_{\mathrm{pinch\text{-}off}}$.

The other two starting plumes generated under the same conditions produced qualitatively and quantitatively similar results. The various vortex ring quantities that were measured are summarized in Table 1.

4
Discussion
A pinch-off process clearly takes place for a starting buoyant plume. At late times, the starting plume's cap achieved an approximately constant circulation, indicating that the stem, or trailing plume, was no longer providing additional circulation to the vortex ring. This pinch-off was observed to occur in a narrow range of non-dimensional times, or formation numbers, between 4.4 and 4.9.

Pinch-off has previously been observed only for vortex rings produced in starting jets using a piston–cylinder apparatus. The starting buoyant plume pinch-off process appears to be closely related to the piston–cylinder pinch-off process. The only major difference between the two processes is that vorticity is produced throughout the flow for the starting buoyant plume, because of acceleration by the buoyancy force, while vorticity production is restricted to the inlet for the starting jet. The observed pinch-off for a starting buoyant plume therefore indicates that the dynamics relating to pinch-off, and to vortex ring formation in general, are not specific to the type of flow that produces the vortex ring. Indeed, aspects of the pinch-off process may be common to all methods of vortex ring formation.

The details of the observed pinch-off are consistent with a model based upon the Kelvin–Benjamin variational principle. According to the Kelvin–Benjamin variational principle, as the fluid in the starting plume at pinch-off is reorganized into a single vortex ring, its energy must increase. This requires that the non-dimensional energy of the forming vortex ring at pinch-off α_{po} is less than α_{vr}. In the Shusser and Gharib (2000b) model, pinch-off occurs when the non-dimensional energy of the trailing plume
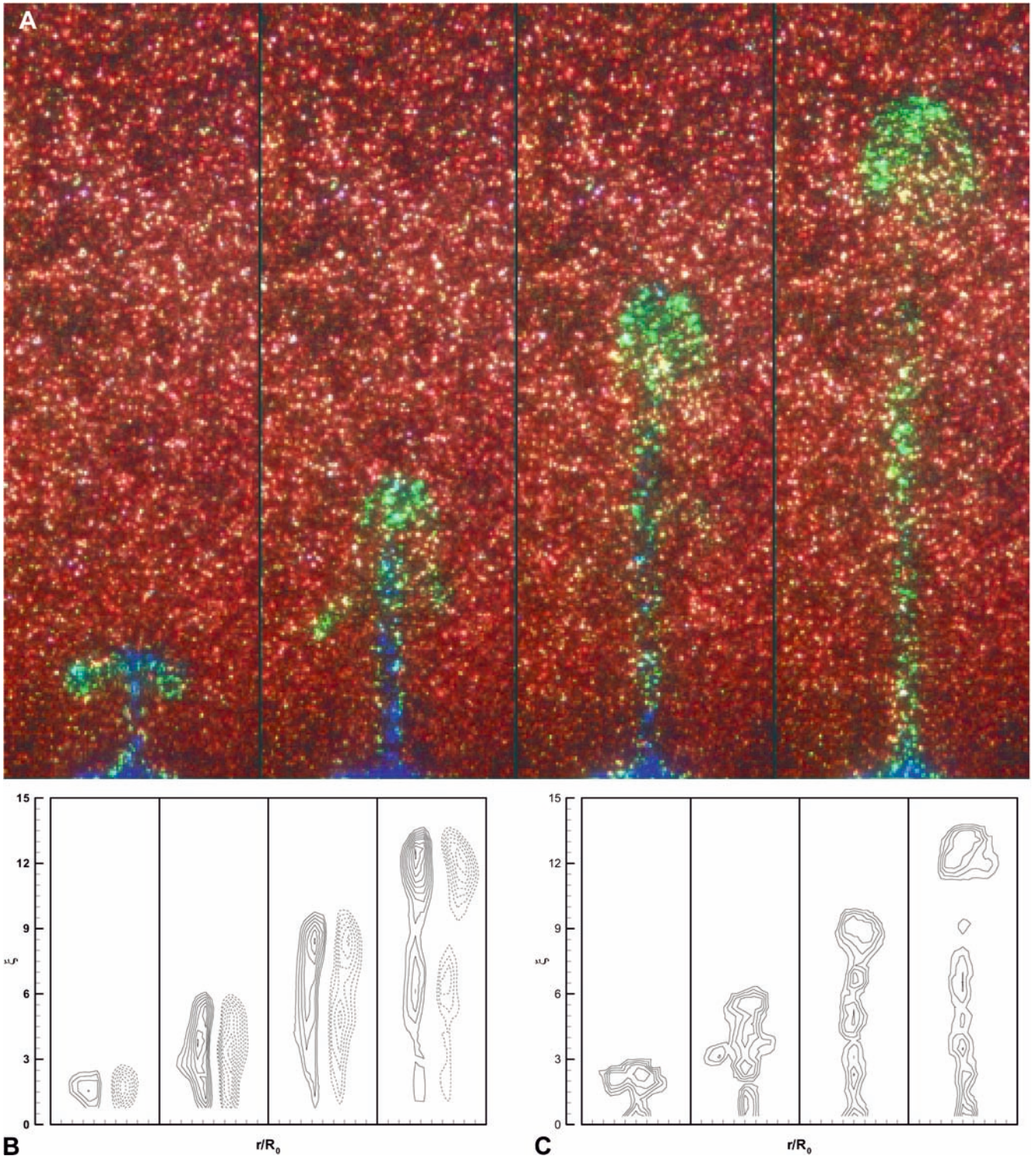
Fig. 2a–c. Snapshots of the flow at non-dimensional times of 2.58, 5.17, 7.77, and 10.36. **a** Images of the starting plume, brightened to improve visibility and cropped horizontally to show the region of interest; **b** vorticity contours; **c** temperature contours

equals the energy of the forming vortex ring, $\alpha_{trail}=\alpha_{po}$. The model therefore requires that $\alpha_{trail}<\alpha_{vr}$ at $\tau_{pinch-off}$ and that pinch-off occurs after the time at which $\alpha_{trail}=\alpha_{vr}$, because $d\alpha_{trail}/d\tau<0$.

In this experiment, α_{tot} was measured, not α_{trail}. While the definition of α (Eq. 6) does not imply that $\alpha_{tot}=\alpha_{trail}$ when $\alpha_{trail}=\alpha_{po}$, it is reasonable to assume that the values

of α_{tot} and α_{trail} are similar at pinch-off. The value of α_{tot} fell below α_{vr} prior to the pinch-off time, which implies that α_{trail} was less than α_{vr} when pinch-off occurred. This is consistent with the model of the pinch-off process based upon the Kelvin–Benjamin variational principle.

There are several significant differences between the conditions in this experiment and those considered in the
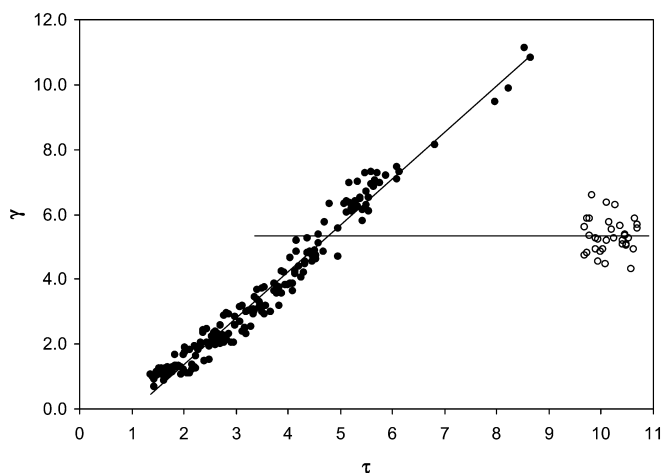
Fig. 3. Non-dimensional circulation as a function of non-dimensional time for the total starting plume (*solid circle*) and for the vortex ring only (*open circle*). A linear fit to the total starting plume data points and the average of the vortex ring data points are shown as *solid lines*
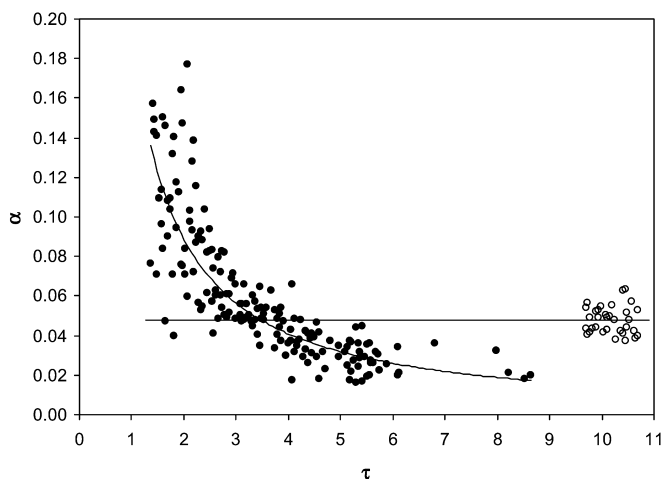

Fig. 4. Non-dimensional energy, α, as a function of non-dimensional time for the total starting plume (*solid circle*) and for the vortex ring only (*open circle*). A polynomial fit to the total starting plume data points and the average of the vortex ring data points are shown as solid lines

Shusser and Gharib (2000b) model, making a direct comparison of the quantitative results inappropriate. However, these differences can be used to identify aspects of the model that must be refined in order to make it useful as a predictive tool. First, the initial conditions for the starting plume are very different in the experiment than in the model. The buoyant fluid in the experiment is produced by a heat source, while in the model the initial mass of buoyant fluid is generated instantaneously. Also, the data that Shusser and Gharib incorporated into their model is from an experiment in which fluid of different density is allowed to enter the ambient fluid by the bursting of a diaphragm (Lundgren et al. 1992). This is more like a thermal than a starting plume. Second, the role of viscous dissipation, entrainment and mixing in the flow must be considered. These processes are explicitly

Table 1. Various quantities measured for the vortex ring produced by a starting buoyant plume for the three separate cases. The quantities are the non-dimensional circulation, pinch-off time, energy and velocity, and the ratio of kinetic energy to the product of velocity and impulse

Run	γ	$\tau_{\text{pinch off}}$	α	u	e/iu
1	5.5±0.6	4.9±0.7	0.050±0.008	1.2±0.1	0.18±0.11
2	5.3±0.5	4.8±0.7	0.048±0.007	1.4±0.1	0.12±0.05
3	5.3±0.6	4.4±0.8	0.048±0.008	1.3±0.2	0.11±0.04

disregarded in the Shusser and Gharib (2000b) model. The Reynolds number for this experiment is quite small ($\Gamma/\nu \approx 86$), so dissipation is likely to play an important role. From the observed temperature fields in Fig. 2c, it is evident that entrainment and mixing are taking place. As the buoyant fluid mixes with the ambient fluid, some of the available gravitational potential energy is lost, so it cannot be completely converted to kinetic energy as the model assumes.

In addition to capturing the vortex ring pinch-off process, the data in this experiment contains information about entrainment and mixing taking place in the flow. For example, several significant features are evident in the temperature and vorticity contours shown in Fig. 2b and c. The vorticity in the plume stem is not distributed uniformly, but rather rolls up into local vortices. The temperature is also not distributed uniformly in the stem. Instead, hot spots are observed to exist, and the locations of these hot spots are related to the location of vorticity concentrations. This indicates that the roll-up of the shear layers in the stem is an important part of the entrainment process. In the plume cap, while there is a location of maximum vorticity, there is no distinct core. This is consistent with the observations of Tanny and Shlien (1985) and is a result of the vortex ring entraining fluid from the plume stem rather than from the ambient fluid. Also, the temperature gradient is steep at the leading edge of the plume, indicating that entrainment is not taking place in this region. This is consistent with the observations of Chay and Shlien (1986) and of Moses et al. (1993). Because the velocity and temperature fields were measured simultaneously in this experiment, it is possible with the existing data to determine the convective heat flux at any point in the flow, within the spatial resolution of the DPITV technique. Using this information, a detailed study of mixing and entrainment could be performed, but that is beyond the scope of this paper.

5
Conclusions

Experiments were conducted in order to study the vortex ring formation process in a starting buoyant plume. The vortex ring pinched-off from the trailing plume—it ceased to entrain additional circulation from the trailing plume and a gap developed between them. Pinch-off was observed to occur at non-dimensional times between 4.4 and 4.9. The details of the pinch-off process are consistent with the Kelvin–Benjamin variational principle and with the basic predictions of Shusser and Gharib (2000b). Additional work focusing on initial conditions, dissipation,

mixing and entrainment is required to create a predictive model of vortex ring pinch-off in starting buoyant plumes.

The starting buoyant plume pinch-off process is similar to that of a vortex ring generated using a piston–cylinder apparatus. The similarity between these processes suggests that pinch-off is a common phenomenon relevant to all vortex rings, regardless of the manner in which they are produced.

References

Benjamin TB (1976) The alliance of practical and analytical insights into the non-linear problems of fluid mechanics. In: Germain P, Nayroles B (eds) Applications of methods of functional analysis to problems in mechanics. Lecture Notes in Mathematics, Vol 503. Springer, Berlin Heidelberg New York, pp 79–166

Chay A, Shlien DJ (1986) Scalar field measurements of a laminar starting plume cap using digital processing of interferograms. Phys Fluids 29:2358–2366

Dabiri D, Gharib M (1991) Digital particle image thermometry: the method and implementation. Exp Fluids 11:77–86

Fay JA (1973) Buoyant plumes and wakes. Ann Rev Fluid Mech 5:151–160

Fernando HJS, Chen R-R, Ayotte BA (1998) Development of a point plume in the presence of background rotation. Phys Fluids 10:2369–2383

Gharib M, Rambod E, Shariff K (1998) A universal time scale for vortex ring formation. J Fluid Mech 360:121–140

Johari H, Gharib M (1998) Near field development of starting buoyant flows. In: Carlomango GM, Grant I (eds) Proceedings of the 8th International Symposium on Flow Visualization, Sorrento, Italy, pp 83.1–83.7

Kelvin L (1880) Vortex statics. Phil Mag 10:97–109

Klein EJ (1968) Application of liquid crystal to boundary layer flow visualization. AIAA Paper No 68-376

List EJ (1982) Turbulent jets and plumes. Ann Rev Fluid Mech 14:189–212

Lundgren TS, Yao J, Mansour NN (1992) Microburst modelling and scaling. J Fluid Mech 239:461–488

McKenna SP, McGillis WR (2002) Performance of digital image velocimetry processing techniques. Exp Fluids 32:106–115

Mohseni K, Gharib M (1998) A model for universal time scale of vortex ring formation. Phys Fluids 10:2436–2438

Morton BR, Taylor G, Turner JS (1956) Turbulent gravitational convection from maintained and instantaneous sources. Proc R Soc A 234:1–23

Moses E, Zocchi G, Libchaber A (1993) An experimental study of laminar plumes. J Fluid Mech 251:581–601

Park HG (1998) A study of heat transfer processes in the wake of a stationary and oscillating circular cylinder using digital particle image velocimetry/thermometry. PhD thesis, California Institute of Technology

Park HG, Dabiri D, Gharib M (2001) Digital particle image velocimetry/thermometry and application to the wake of a heated circular cylinder. Exp Fluids 30:327–338

Parsley M (1991) The Hallcrest handbook of thermochromic liquid crystal technology. Hallcrest, Glenview, IL

Rast MP (1998) Compressible plume dynamics and stability. J Fluid Mech 369:125–149

Rhee HS, Koseff JR, Street RL (1984) Flow visualization of a recirculating flow by rheoscopic liquid and liquid crystal techniques. Exp Fluids 2:57–64

Shusser M, Gharib M (2000a) Energy and velocity of a forming vortex ring. Phys Fluids 12:618–621

Shusser M, Gharib M (2000b) A model for vortex ring formation in a starting buoyant plume. J Fluid Mech 416:173–185

Tanny J, Shlien DJ (1985) Velocity field measurements of a laminar starting plume. Phys Fluids 28:1027–1032

Turner JS (1957) Buoyant vortex rings. Proc R Soc A 239:61–75

Turner JS (1962) The "starting plume" in neutral surroundings. J Fluid Mech 13:356–368

Willert CE, Gharib M (1991) Digital particle image velocimetry. Exp Fluids 10:181–193

94